AIP | Journal of Applied Physics

Superstrong coupling of thin film magnetostatic waves with microwave cavity

Xufeng Zhang, Changling Zou, Liang Jiang, and Hong X. Tang

Citation: Journal of Applied Physics **119**, 023905 (2016); doi: 10.1063/1.4939134
View online: http://dx.doi.org/10.1063/1.4939134
View Table of Contents: http://scitation.aip.org/content/aip/journal/jap/119/2?ver=pdfcov
Published by the AIP Publishing

JOURNAL OF APPLIED PHYSICS 119, 023905 (2016)

Superstrong coupling of thin film magnetostatic waves with microwave cavity

Xufeng Zhang,[1] Changling Zou,[1,2] Liang Jiang,[2] and Hong X. Tang[1,a)]
[1]Department of Electrical Engineering, Yale University, New Haven, Connecticut 06511, USA
[2]Department of Applied Physics, Yale University, New Haven, Connecticut 06511, USA

(Received 22 September 2015; accepted 16 December 2015; published online 13 January 2016)

We experimentally demonstrated the strong coupling between a microwave cavity and standing magnetostatic magnon modes in a yttrium iron garnet film. Such strong coupling can be observed for various spin wave modes under different magnetic field bias configurations, with a coupling strength inversely proportional to the transverse mode number. A comb-like spectrum can be obtained from these high order modes. The collectively enhanced magnon-microwave photon coupling strength is comparable with the magnon free spectral range and therefore leads to the superstrong coupling regime. Our findings pave the road towards designing a new type of strongly hybridized magnon-photon system. © *2016 AIP Publishing LLC*.
[http://dx.doi.org/10.1063/1.4939134]

I. INTRODUCTION

Magnonics, which studies the collective spin excitation in magnetic materials, has been attracting intensive attentions recently because of its great potential in constructing hybrid systems.[1] As an information carrier, magnon utilizes a new degree of freedom—the electron spin, which provides various unique properties distinct from conventional information carriers. For instance, unlike electronic charges, magnon is free of Ohmic loss when propagating in magnetic insulators because there are no itinerant electrons evolved.[2] Since the spin degree of freedom is more isolated from the environment, magnon suffers less from the environmental perturbation and usually has long lifetime. Moreover, since the magnon frequency is determined by the bias magnetic field, it can be tuned in a wide frequency range from several GHz to 100 GHz. Among all magnon media, ferrimagnetic insulator yttrium iron garnet (YIG) shows the lowest magnetic damping[3,4] and therefore is widely used.[2,5–12] Aside from its outstanding magnetic and microwave properties, YIG also possesses excellent mechanical and optical properties, making it an ideal platform for system integration.

Very recently, strong coupling between the magnon in YIG spheres and three dimensional microwave cavity photons was demonstrated by several groups.[13–19] Thanks to the large spin density in YIG, the coupling strength g between magnon and microwave photon is collectively enhanced by a factor of $\sqrt{N}$, where N is the total spin number.[20,21] Strong coupling regime $g \gg \kappa_{c,m}$ is demonstrated[13–19] (κ_m and κ_c are the linewidths of magnon and cavity microwave photon, respectively), indicating that the information can be exchanged between the two systems multiple times before getting dissipated, which makes the magnon-based coherent information processing possible. With specially designed cavities, the coupling strength g can be further increased to reach the ultrastrong coupling regime, where the coupling strength is comparable with the transition frequency ($g \gtrsim 0.1\omega_0$).[15,16]

However, previously studied hybrid microwave-magnon systems are always focusing on the ferromagnetic resonance (FMR) of the YIG spheres. In this most simple case, all the spins in the YIG sphere precess in phase, and therefore the whole YIG sample can be treated as a giant spin. Considering the near-uniform microwave cavity field, only the FMR mode can be effectively excited in small YIG spheres. When the YIG sphere size increases such that the microwave cavity field can no longer be treated as uniform, high order magnon modes can also be accessed. In a YIG sphere, there exist a large amount of high order modes, yielding a very complicated spectrum when they couple with the microwave cavity resonance.[15,16,22,23] These high order modes in YIG spheres are difficult to be selected for practical use.

In this work, we study the coherent magnon-photon coupling using a thin film YIG sample[13,24–26] instead of sphere geometry inside a three dimensional (3D) microwave cavity. It is well known that in YIG thin films there exist magnetostatic waves whose dispersion relations are distinctly different from those in bulk YIG. Depending on the direction of the bias magnetic field, the film normal direction, and the wave propagation direction, there exist three different magnetostatic modes, noted as the forward volume magnetostatic wave (FVMSW), backward volume magnetostatic wave (BVMSW), and magnetostatic surface wave (MSSW).[7,27–29] Unlike the FMR modes in a YIG sphere, all these modes have nonuniform field distribution and non-zero wave vector in YIG thin films. As a result of the lateral confinement due to the finite width of the YIG film,[30] these propagating magnetostatic waves form almost evenly distributed standing wave modes in the YIG thin film with a free-spectral range (FSR) determined by the film dimension. We found that the coupling strength of the high-order magnon modes (standing waves) with the cavity resonance is comparable to the FSR, leading to a new coherent interaction

a)Electronic mail: hong.tang@yale.edu

regime: the superstrong coupling regime.[31–34] Within this regime, the eigenmodes of the thin film are significantly changed by the vacuum cavity field, giving rise to magnon hybridization. Using thin film geometry, a single sample can provide multiple modes which are individually addressable for signal processing, showing great potential for nonlinear magnon conversion and memory.[19] More intriguingly, such a system can be further integrated with other planar electronic and optical devices and therefore is a very promising candidate as an information transducer that connects MHz, GHz, and THz frequencies.

II. EXPERIMENT SETUP

The device used in our experiments consists of one 3D microwave cavity and one piece of single-crystal YIG thin film. The microwave cavity, which is machined from high conductivity copper, has a dimension of $43 \times 21 \times 7.1\ \mathrm{mm}^3$ with its TE_{101} mode resonating at 7.88 GHz. The 5-μm-thick YIG thin film is epitaxially grown on a 500-μm-thick gadolinium gallium garnet (GGG) substrate and has a size of $11 \times 2\ \mathrm{mm}^2$. The YIG thin film locates at the maximum microwave magnetic field of the TE_{101} mode, as shown in Fig. 1(a), to maximize the coupling between the magnon and microwave photon. An external bias magnetic field is applied along z direction, perpendicular to the microwave magnetic field which is along x direction, to allow the excitation of the magnon mode in the YIG thin film. With such a configuration, the YIG thin film supports three different magnetostatic modes depending on the orientation of the YIG thin film.[7,27] FVMSW can be exited in a normally magnetized YIG film [film in the xy plane, Fig. 1(b)], whose dispersion is described as

$$f_F = \sqrt{f_H\left[f_H + f_M\left(1 - \frac{1 - e^{-kd}}{kd}\right)\right]}, \tag{1}$$

while BVMSW and MSSW can be excited in a parallelly magnetized YIG thin film [film in xz or yz plane, Figs. 1(c) and 1(d)], whose dispersion relations are given by

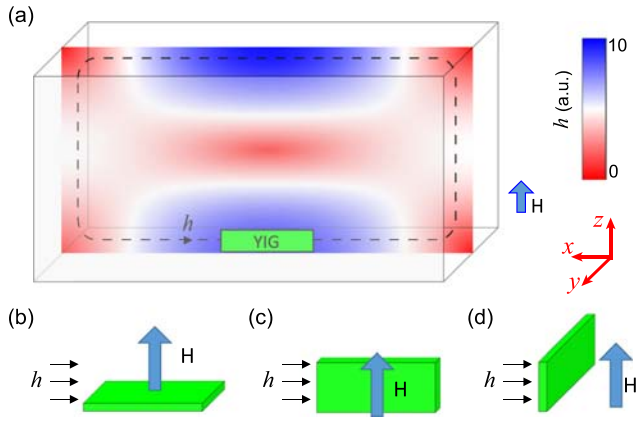

FIG. 1. (a) Sketch of the microwave cavity with a YIG thin film on the inside wall. H: external bias magnetic field; h: microwave magnetic fields. Intensity map shows the magnetic field distribution of the micrwave resonance (TE_{101} mode). (b)–(d) Schematics of different film orientations.

$$f_B = \sqrt{f_H\left(f_H + f_M\frac{1 - e^{-kd}}{kd}\right)}, \tag{2}$$

$$f_S = \sqrt{\left(f_H + \frac{f_M}{2}\right)^2 - \left(\frac{f_M}{2}\right)^2 e^{-2kd}}, \tag{3}$$

respectively. Here, $f_M = \gamma 4\pi M_S$, $f_H = \gamma H_0$, $4\pi M_S$ is the saturation magnetization, H_0 is the effective magnetic field, f_c is the cavity resonance frequency, γ is the gyromagnetic ratio, k is the wave vector, and d is the thickness of the YIG film.

For the perpendicularly magnetized YIG film, the excited FVMSWs can propagate along any in-plane directions. In the parallel magnetization situation, the excited waves propagating in the direction parallel to the bias magnetic field are BVMSWs, while those propagating perpendicular to the bias magnetic field are the MSSWs. These magnetostatic modes coherently couple with the cavity resonance via magnetic dipole-dipole interaction, and strong coupling can be achieved as a result of the large spin density of YIG.

III. SPECTRUM OF THIN FILM MAGNONS

The coupling between the cavity resonance and the magnon modes is characterized by measuring the reflection from the cavity using a vector network analyzer via a coaxial probe. The magnon frequency is swept by tuning the bias magnetic field, and when it crosses the microwave resonance frequency, the magnons couple with the cavity photons. With a total number of 4.64×10^{17} spins in our YIG thin film sample, the magnon-photon coupling is significantly enhanced.

We start with measuring the spectrum of the magnon modes in the thin film using a low-Q cavity. Microwave absorber is placed inside the copper cavity to reduce its Q factor to around 10, which also slightly lowers the cavity resonance frequency. Figure 2 shows the typical reflection spectra at varying magnetic field for the in-plan magnetized YIG

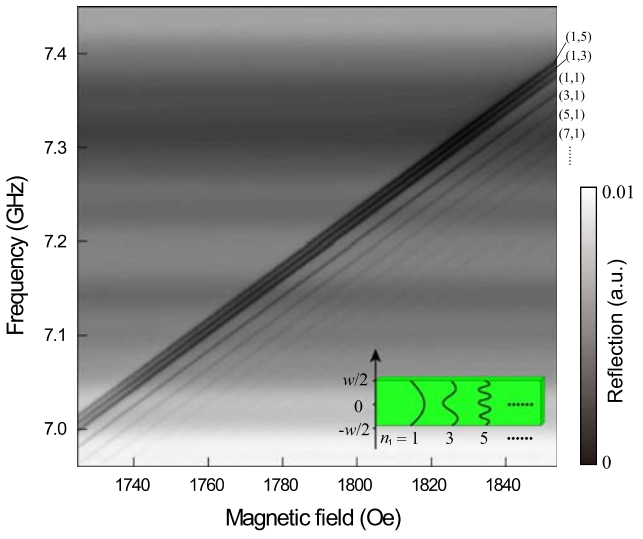

FIG. 2. Reflection spectrum of a device with an in-plane magnetized YIG thin film and a large cavity resonance linewidth. The cavity resonance is indistinguishable from the background due to its large linewidth. Each mode is labeled with its mode number (n_1,n_2). Inset: Schematic illustration of the BVMSW standing modes with odd mode number n_1 in a YIG thin film with width w.

film. Due to the large linewidth of the cavity resonance and the under coupling condition from the coaxial probe, the magnon resonances show up in the measured reflection spectra as absorption dips.[15] For an in-plane magnetized YIG film, the two different orientations as shown in Figs. 1(c) and 1(d) give almost identical results in our experiments, since the direction of the excitation microwave field with respect to the film plane does not affect the magnon-photon coupling. Although the magnons are excited in a continuous band, the finite film size leads to the formation of discrete standing wave modes confined by the film edges,[30,35,36] which correspond to the resonance dips in Fig. 2. These standing wave modes are BVMSWs, each characterized by their wave number (n_1, n_2), where n_1 and n_2 are the wave number along the width and length directions, respectively. The according wave vectors can be calculated as $k_1 = n_1 \times \pi/w$ and $k_2 = n_2 \times \pi/l$, where w and l are the width and length of the YIG film, respectively. The two groups of resonance lines in Fig. 2 correspond to high order modes along the two orthogonal directions: The modes with larger spacing (18.1 MHz) are high order modes along the width direction, while those with relatively small spacing (7.4 MHz) are high order modes along the length direction. Note as the mode order along the length direction (n_2) becomes larger, the magnon modes change from BVMSW to MSSW.[35,37] Since the MSSWs are localized at the film surface and exponentially decay into the film, they have much smaller mode overlap with the cavity mode which in turn leads to much weaker coupling. This may explain why we only observed two high order modes along the length direction. When we repeat the measurement with out-of-plane magnetization, similar spectrum can be observed for the MSFVM. However, for the MSFVM the two orthogonal in-plane directions are identical, so the high order modes along these two directions fall in the same frequency range and overlap with each other, making it difficult to distinguish each individual mode from the spectrum. This explains the much cleaner spectrum in Fig. 3 for the BVMSW compared with the FVMSW. For both in-plane and out-of-plane magnetizations, only modes with odd mode numbers can be detected because those with even mode numbers have cancelled coupling strength with the uniform cavity field.

To study the strong magnon-photon coupling, we place the film in a high-Q microwave cavity ($Q = 2690$). Since the fundamental modes along the length direction ($n_2 = 1$) have the largest coupling strength with the cavity mode, we only focus on these modes and ignore the high order modes along this direction ($n_2 \geq 3$). In contrast to the uniformly distributed resonance lines in Fig. 2, in a high-Q cavity the coherent magnon-photon coupling gives rise to strongly modified spectrum when magnons are near resonance with the cavity resonance, as indicated by the anti-crossing features in the measured reflection spectra in Figs. 3(a) and 3(b).

From the measured spectra, we are able to identify the magnon mode order for each anti-crossing, considering the fundamental (1,1) mode always has the largest coupling strength, as will be shown later. A distinct difference between the two spectra shown in Fig. 3 is that the fundamental mode has the highest bias magnetic field in (a) while it is the lowest in (b). This can be explained by the opposite slope of their dispersion relations, which can be obtained by extracting the frequencies of each crossing point [Fig. 3(c)]. The measured dispersion relations show great agreement with theoretical fittings using Eqs. (1) and (2). Note that the effective internal magnetic field in the YIG film $H_0 = H - 4\pi M_S$ for the perpendicular magnetization, while $H_0 = H$ for the in-plane magnetization (H is the externally applied bias field), which explains why the FVMSW resonates at higher bias fields than the BVMSW for a given frequency.

IV. SUPERSTRONG COUPLING

We extract the coupling strength for each anti-crossing in the spectra in Fig. 3, and plot them as a function of mode order in Fig. 4, which shows a clear inverse proportional dependence. Theoretically, since the magnon-photon coupling strength is proportional to the mode overlapping between the magnon and cavity modes, it can be explicitly expressed as[15]

$$g_{n1} = \frac{\sin\frac{n_1\pi}{2}\eta}{2n_1\pi}\gamma\sqrt{\frac{2\pi\hbar f_a\mu_0}{V_a}}\sqrt{2Ns}, \tag{4}$$

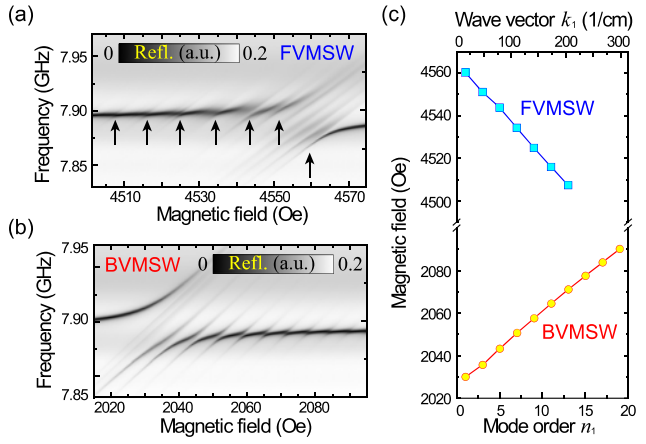

FIG. 3. Measured reflection spectrum for the device with perpendicularly (a) and in-plane (b) magnetized YIG thin film. Arrows in (a) are to help identify the resonance points. (c) Extracted (symbols) and calculated (solid lines) dispersions for the two magnon modes.

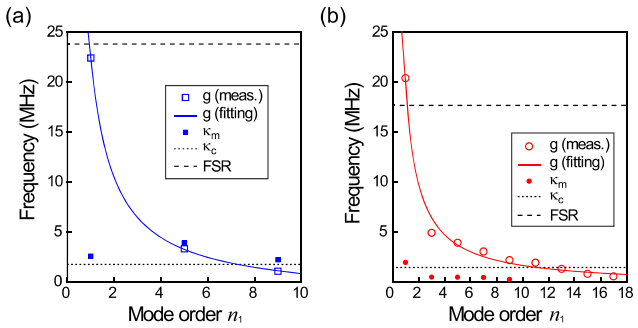

FIG. 4. Coupling strength g, magnon linewidth κ_m, cavity linewidth κ_c, and magnon FSR as a function of mode order n for the FVMSW (a) and the BVMSW (b), respectively.

for the magnon mode with mode number $(n_1, 1)$. Here, $\hbar$ is the reduced Planck's constant, f_a and V_a are the frequency and mode volume of the microcavity resonance, μ_0 is the vacuum permeability, $N = \rho_s V_{\mathrm{YIG}}$ is the total number of spins in YIG with spin density $\rho_s = 4.22 \times 10^{27}\,\mathrm{m}^{-3}$, and $s = 5/2$ is the ground state spin number of YIG. The factor $\eta \leq 1$ accounts for the effect of imperfect spatial overlap between the magnon and cavity field, magnetic field alignment and demagnetization effect of thin film. Note we used a sine function for the magnon standing modes (Fig. 2, inset) by considering the pinned boundary condition of dynamic magnetization at the film edges.[30] Clearly an even n_1 leads to a zero integration, indicating a vanished coupling strength between the even modes and the cavity resonance. As a result, the observed resonances in the reflection spectra are all from the odd modes, whose coupling strength with the microwave photons is $|g_{n1}| = g_1/n_1$. Solid lines in Fig. 4 are numerical fittings using such a relation, showing great agreement with the measurement results (symbols) for both the FVMSW and BVMSW.

In Fig. 4, we also plot the extracted cavity and magnon linewidths for comparison. Clearly for both the FVMSW and the BVMSW, the coupling strength of the lower order magnon modes with the cavity photons already exceeded the cavity and magnon linewidth, indicating that the coherent magnon-photon coupling has reached the strong coupling regime. Particularly, for the BVMSW modes, strong coupling can be achieved for up to the 9th order magnon mode.

In general, the mode splitting at the anti-crossing is a direct indication of the coupling strength $(\Delta f = 2g)$. However, in the thin film situation where multiple modes simultaneously couple with the cavity resonance, the mode splitting no longer directly reflects the coupling strength if the free spectral range (FSR) of the magnon modes is comparable with the coupling strength, which is known as the *superstrong coupling regime*.[31–34] Such a new coupling regime is very interesting in both fundamental study and practical applications. In a YIG thin film in free-space, different magnon modes are orthogonal with each other. But when they are superstrongly coupled with a high-Q microwave cavity, the profiles and properties of each magnon mode are greatly modified by the vacuum electromagnetic field. In Fig. 4, we also plot the measured FSR of the corresponding magnon modes as a comparison. It is evident that our system has entered the superstrong coupling regime as the magnon-photon coupling strength is, indeed, comparable or even larger than the magnon FSR both for the FVMSW and the BVMSW. Via sophisticated cavity design which can further reduce the cavity mode volume and concentrate the resonance field,[16] the coupling strength between magnon and microwave photon can be further increased and therefore $g \gg$ FSR is achievable, which can lead us deep into the superstrong coupling regimes.

V. CONCLUSION

In summary, we demonstrated the coherent coupling between microwave photons with various magnetostatic resonances in a thin film geometry. We found that the coupling strength is inversely proportional to the transverse mode order, which is confirmed with both theoretical calculation and experimental data. Strong coupling is achieved thanks to the large spin number in the YIG, and moreover, even the superstrong coupling is demonstrated where the coupling strength is comparable with the magnon FSR. Aside from demonstrating a new coupling regime, our system also shows a great potential in practical applications. For instance, the YIG thin film provides a series of standing wave magnon resonances, which allows us to build an evenly distributed resonance array in a single YIG device whose physical size can be much smaller than the wavelength, providing great opportunities in applications such as memory and comb generation. Our results move one step further compared with the widely used hybrid microwave systems that utilize ferromagnetic resonances, and pave the way toward building low loss hybridized system.

ACKNOWLEDGMENTS

This work was supported by DARPA/MTO MESO program. H.X.T. and L.J. acknowledge supports from Packard Fellowship in Science and Engineering.

[1]G. Kurizki, P. Bertet, Y. Kubo, K. Mølmer, D. Petrosyan, P. Rabl, and J. Schmiedmayer, Proc. Natl. Acad. Sci. U.S.A. **112**, 3866 (2015).
[2]Y. Kajiwara *et al.*, Nature **464**, 262 (2010).
[3]E. G. Spencer, R. C. LeCraw, and A. M. Clogston, Phys. Rev. Lett. **3**, 32 (1959).
[4]E. G. Spencer, R. C. LeCraw, and R. C. Linares, Phys. Rev. **123**, 1937 (1961).
[5]A. V. Chumak, A. A. Serga, and B. Hillebrands, Nat. Commun. **5**, 4700 (2014).
[6]B. Lenk, H. Ulrichs, F. Garbs, and M. Münzenberg, Phys. Rep. **507**, 107 (2011).
[7]A. A. Serga, A. V. Chumak, and B. Hillebrands, J. Phys. D: Appl. Phys. **43**, 264002 (2010).
[8]D. Qu, S. Y. Huang, J. Hu, R. Wu, and C. L. Chien, Phys. Rev. Lett. **110**, 067206 (2013).
[9]T. An *et al.*, Nat. Mater. **12**, 549 (2013).
[10]T. Satoh, Y. Terui, R. Moriya, B. A. Ivanov, K. Ando, and E. Saitoh, Nat. Photonics **6**, 662 (2012).
[11]M. Wu, B. A. Kalinikos, and C. E. Patton, Phys. Rev. Lett. **95**, 237202 (2005).
[12]A. Slavin and I. Rojdestvenski, IEEE Trans. Magn. **30**, 37 (1994).
[13]H. Huebl, C. Zollitsch, J. Lotze, F. Hocke, M. Greifenstein, A. Marx, R. Gross, and S. Goennenwein, Phys. Rev. Lett. **111**, 127003 (2013).
[14]Y. Tabuchi, S. Ishino, T. Ishikawa, R. Yamazaki, K. Usami, and Y. Nakamura, Phys. Rev. Lett. **113**, 083603 (2014).
[15]X. Zhang, C.-L. Zou, L. Jiang, and H. X. Tang, Phys. Rev. Lett. **113**, 156401 (2014).
[16]M. Goryachev, W. G. Farr, D. L. Creedon, Y. Fan, M. Kostylev, and M. E. Tobar, Phys. Rev. Appl. **2**, 054002 (2014).
[17]L. Bai, M. Harder, Y. P. Chen, X. Fan, and J. Q. Xiao, Phys. Rev. Lett. **114**, 227201 (2015).
[18]Y. Tabuchi, S. Ishino, A. Noguchi, T. Ishikawa, R. Yamazaki, K. Usami, and Y. Nakamura, Science **349**, 405 (2015).
[19]X. Zhang, C.-L. Zou, N. Zhu, F. Marquardt, L. Jiang, and H. X. Tang, Nat. Commun. **6**, 8914 (2015).
[20]M. Raizen, R. Thompson, R. Brecha, H. Kimble, and H. Carmichael, Phys. Rev. Lett. **63**, 240 (1989).
[21]D. F. Walls and G. J. Milburn, *Quantum Optics* (Springer, Berlin, 1994).
[22]B. Zare Rameshti, Y. Cao, and G. E. W. Bauer, Phys. Rev. B **91**, 214430 (2015).
[23]N. J. Lambert, J. A. Haigh, and A. J. Ferguson, J. Appl. Phys. **117**, 053910 (2015).
[24]G. B. G. Stenning, G. J. Bowden, L. C. Maple, S. A. Gregory, A. Sposito, R. W. Eason, N. I. Zheludev, and P. A. J. de Groot, Opt. Express **21**, 1456 (2013).

[25]Y. Cao, P. Yan, H. Huebl, S. T. B. Goennenwein, and G. E. W. Bauer, Phys. Rev. B **91**, 094423 (2015).
[26]B. Bhoi, T. Cliff, I. S. Maksymov, M. Kostylev, R. Aiyar, N. Venkataramani, S. Prasad, and R. L. Stamps, J. Appl. Phys. **116**, 243906 (2014).
[27]D. D. Stancil and A. Prabhakar, *Spin Waves - Theory and Applications* (Springer, Boston, MA, 2009).
[28]M. Hurben and C. Patton, J. Magn. Magn. Mater. **139**, 263 (1995).
[29]M. Hurben and C. Patton, J. Magn. Magn. Mater. **163**, 39 (1996).
[30]K. Y. Guslienko, S. O. Demokritov, B. Hillebrands, and A. N. Slavin, Phys. Rev. B **66**, 132402 (2002).
[31]D. Meiser and P. Meystre, Phys. Rev. A **74**, 065801 (2006).
[32]X. Yu, D. Xiong, H. Chen, P. Wang, M. Xiao, and J. Zhang, Phys. Rev. A **79**, 061803 (2009).
[33]N. M. Sundaresan, Y. Liu, D. Sadri, L. J. Szöcs, D. L. Underwood, M. Malekakhlagh, H. E. Türeci, and A. A. Houck, Phys. Rev. X **5**, 021035 (2015).
[34]N. Kostylev, M. Goryachev, and M. E. Tobar, e-print arXiv:1508.04967 (2015).
[35]B. E. Storey, A. O. Tooke, A. P. Cracknell, and J. A. Przystawa, J. Phys. C **10**, 875 (1977).
[36]R. Gieniusz, J. Magn. Magn. Mater. **119**, 187 (1993).
[37]B. Tittmann, Solid State Commun. **13**, 463 (1973).